thank R. D. Chapman (University California, Irvine) for his assistance in the structure determination and M. J. Root (University of Cincinnati) for his assistance with the alkylation experiment.

Registry No. $[(en)_2Co(SC_6H_4NH_2)](ClO_4)_2$, 72905-17-0; $[(en)_2Co(S(O)C_6H_4NH_2)](ClO_4)_2$, 72893-80-2; $[(en)_2Co(S(O)_2C_6H_4NH_2)](ClO_4)_2$, 72893-82-4; $[(en)_2Co(S(O)_2C_6H_4NH_2)](SCN)_2$, 72893-84-6; 2,2′-diaminodiphenyl disulfide, 1141-88-4; $[(en)_2Co(SC_6H_4NH_2)](ClO_4)Cl$, 72905-18-1.

Supplementary Material Available: Listings of structure factor amplitudes, hydrogen atom positional parameters, and principal root-mean-square amplitudes of thermal motion (11 pages). Ordering information is given on any current masthead page.

Contribution from the Faculty of Pharmaceutical Science, Kyoto University, Shimoadachi-cho, Yoshida, Sakyo-ku, Kyoto, Japan, and the Department of Synthetic Chemistry, Kyoto University, Honmachi, Yoshida, Sakyo-ku, Kyoto, Japan

Crystal and Molecular Structure of (Octaethylporphinato)iron(III) Perchlorate. Anomalous Magnetic Properties and Structural Aspects

HIDEKI MASUDA,* TOORU TAGA, KENJI OSAKI, HIROSHI SUGIMOTO, ZEN-ICHI YOSHIDA, and HISANOBU OGOSHI*

Received August 6, 1979

The crystal structure of (octaethylporphinato)iron(III) perchlorate has been determined by the X-ray method. The compound crystallizes in the monoclinic space group $P2_1/a$ with four molecules in a unit cell of dimensions a = 18.87 (1) Å, b = 14.20 (5) Å, c = 13.64 (1) Å, and β = 106.05 (6)°. The crystal structure is composed of dimers of the complex; the two iron porphyrins have a "face-to-face" contact with a closest approach of 3.56 Å between the meso carbon and the pyrrolic α-carbon on the different porphyrins. This dimerization is explained by weak π–π^* interactions. Weak (π-pyrrolyl)iron interactions were also noted between the approached complexes. The perchlorate anion has C_{3v} symmetry. Fe→(O_1–Cl) π^* back-bonding seems to cause a longer Cl–O_1 bond (1.515 Å) relative to the other three Cl–O bonds. The porphinato core is planar within 0.04 Å. The average Fe–N and Fe–$OClO_3$ distances are determined as 1.994 (10) and 2.067 (9) Å, respectively. The iron atom is displaced by 0.26 Å out of the plane defined by the four porphinato nitrogen atoms. The overall geometric parameters give a good indication that the complex has an intermediate-spin state ($S = {}^3/_2$) in comparison with high- or low-spin iron porphyrins. The temperature-dependent magnetic moment revealed the iron atom to be in the $S = {}^3/_2$ state only. The structural details are discussed with its anomalous magnetic properties from other physical measurements.

Introduction

Ferricytochrome c', a heme enzyme, isolated from photosynthetic and denitrifying bacteria, has been shown to have unusual chemical and physical properties.[1] Maltempo has suggested that the anomalous magnetic property arises from the electronic configurations of heme iron at the ground state of quantum mechanical admixtures of an intermediate-spin state ($S = {}^3/_2$) and of a high-spin state ($S = {}^5/_2$), coupled via a spin–orbit interaction.[1]

Few intermediate-spin or mixed-spin synthetic heme complexes have received much attention[2-4,6] since the synthesis and magnetic properties of (octaethylporphinato)iron(III) perchlorate, $(OEP)Fe^{III}ClO_4$, were reported.[2,3] The unusual magnetic moments of these complexes were interpreted in terms of a thermal admixture of the high-spin ($S = {}^5/_2$) and low-spin ($S = {}^1/_2$) states.[3] Recently, Dolphin et al.[2] have reported that $(OEP)Fe^{III}ClO_4$ is of an intermediate-spin state on the basis of Mössbauer spectra and magnetic susceptibility at various temperatures. The structure of heme centers has been discussed in relation to the function and mechanism of heme proteins.[5b] A number of molecular structures of iron porphyrins have been reported.[5,8-10] Scheidt et al. have reported the crystal structure of the ferric perchlorate complex of tetraphenylporphine, $(TPP)Fe^{III}ClO_4 \cdot {}^1/_2C_8H_{10}$[6a,b] and interpreted it in terms of the $S = {}^3/_2$ state and the quantum mechanically mixed $S = {}^3/_2, {}^5/_2$ state, respectively. In this paper, we describe the crystal structure of $(OEP)Fe^{III}ClO_4$, its geometry, and its temperature-dependent magnetic moment.

Experimental Section

Crystal Structure. $(OEP)Fe^{III}ClO_4$ was prepared by refluxing a benzene solution of $(OEP)Fe^{III}Cl$ and $AgClO_4$.[3] Dark brown platelike crystals were obtained by recrystallization from benzene solution. Preliminary X-ray data showed that the crystal is monoclinic and the space group is $P2_1/a$ from the systematic absences of $h0l$ for h odd and $0k0$ for k odd. The unit cell dimensions are a = 18.87 (1) Å, b = 14.20 (5) Å, c = 13.64 (1) Å, and β = 106.05 (6)°, from Weissenberg photographs calibrated by Ge standard power lines, respectively. The calculated density, with the assumption of four molecules in a unit cell, is 1.300 g/cm^3. The observed density was

* To whom correspondence should be addressed: H.M., Faculty of Pharmaceutical Science; H.O., Department of Synthetic Chemistry.

(1) (a) Maltempo, M. M. *J. Chem. Phys.* **1974**, *61*, 2540. (b) Maltempo, M. M.; Moss, T. H.; Cusanovich, M. A. *Biochim. Biophys. Acta* **1974**, *342*, 290. (c) Maltempo, M. M. *Ibid.* **1975**, *379*, 97.
(2) Dolphin, D. H.; Sams, J. R.; Tsin, T. B. *Inorg. Chem.* **1977**, *16*, 711.
(3) Ogoshi, H.; Watanabe, E.; Yoshida, Z. *Chem. Lett.* **1973**, 989.
(4) Ogoshi, H.; Sugimoto, H.; Yoshida, Z., submitted for publication.
(5) (a) Hoard, J. R. "Porphyrins and Metalloporphyrins"; Smith, K. M., Ed.; Elsevier: Amsterdam, 1975; Chapter 8. (b) Hoard, J. L. *Science* **1971**, *174*, 1295. (c) Scheidt, W. R. *Acc. Chem. Res.* **1977**, *10*, 339.
(6) (a) Kastner, M. E.; Scheidt, W. R.; Mashiko, T.; Reed, C. A. *J. Am. Chem. Soc.* **1978**, *100*, 666. (b) Reed, C. A.; Mashiko, T.; Bentley, S. P.; Kastner, M. E.; Scheidt, W. R.; Spartalian, K.; Lang, G. *Ibid.* **1979**, *101*, 2948. (c) Scheidt, W. R.; Cohen, I. A.; Kastner, M. E. *Biochemistry* **1979**, *18*, 3546.
(7) (a) Ibers, J. A., Hamilton, W. C., Eds.; "International Tables for X-Ray Crystallography"; Kynoch Press: Birmingham, England, 1974; Vol. IV. (b) Macgillavry, C. H.; Rieck, G. D., Lonsdale, K., Eds. "International Tables for X-Ray Crystallography"; Kynoch Press: Birmingham, England, 1968; Vol. III.
(8) (a) Koenig, D. M. *Acta Crystallogr.* **1965**, *18*, 663. (b) Hoard, J. L; Hamor, M. J.; Hamor, T. A.; Caughey, W. S. *J. Am. Chem. Soc.* **1965**, *87*, 2312. (c) Hoard, J. L.; Cohen, G. N.; Glick, M. D. *Ibid.* **1967**, *89*, 1992. (d) Hoffman, A. B.; Collins, D. M.; Day, V. W.; Fleischer, E. B.; Srivastava, T. S.; Hoard, J. L. *Ibid.* **1972**, *94*, 3620. (e) Mashiko, T.; Kastner, M. E.; Spartalian, K.; Scheidt, W. R.; Reed, C. A. *Ibid.* **1978**, *100*, 6354.
(9) Tang, S. C.; Koch, S.; Papaefthymiou, G. C.; Foner, S.; Frankel, R. B.; Ibers, J. A.; Holms, R. H. *J. Am. Chem. Soc.* **1976**, *98*, 2414.
(10) (a) Collins, D. M.; Countryman, R.; Hoard, J. L. *J. Am. Chem. Soc.* **1972**, *94*, 2066. (b) Takenaka, A.; Sasada, Y.; Ogoshi, H.; Watanabe, E.; Yoshida, Z. *Chem. Lett.* **1972**, 1235. (c) Little, R. G.; Dymoch, K. R.; Ibers, J. A. *J. Am. Chem. Soc.* **1975**, *97*, 4532.
(11) Tulinsky, A.; Chen, B. M. L. *J. Am. Chem. Soc.* **1977**, *99*, 3647.

0020-1669/80/1319-0950$01.00/0 © 1980 American Chemical Society

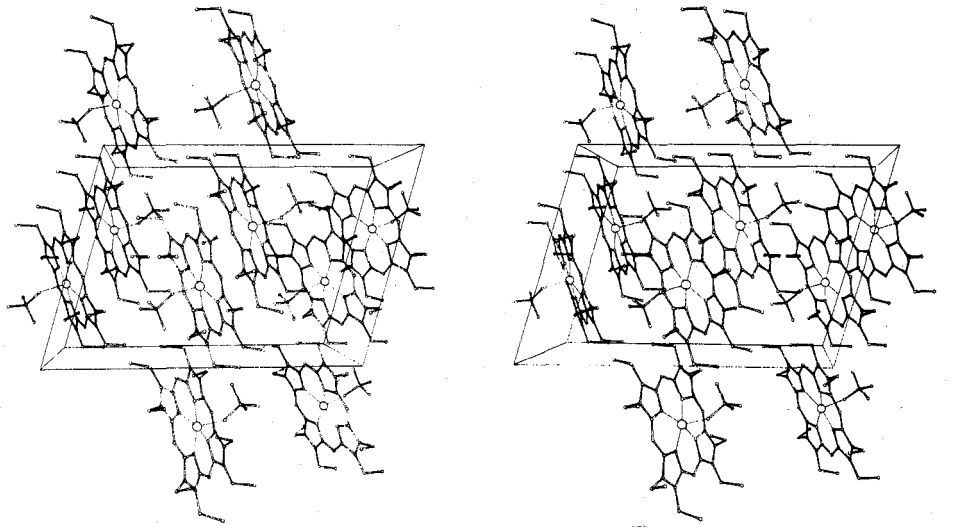

Figure 1. Stereoscopic view of the contents of one unit cell of $(OEP)Fe^{III}ClO_4$. The x axis is horizontal to the right, the y axis is almost vertical, and the z axis is about perpendicular to the paper going up to the reader. Hydrogen atoms have been omitted.

1.287 (2) g/cm^3, measured by flotation in calcium chloride solutions. Equi-inclination Weissenberg photographs were taken by rotating the crystal about the b and c axes by using nickel-filtered Cu Kα radiation. Intensity data were corrected on an AD-1 densitometer collected by a NOVA 1200 computer acting in cooperation with a DIABLO 31 disk drive. Structure factors of 2070 independent reflections were obtained through the usual data reduction procedure. An absorption correction was applied by using the linear absorption coefficient of 45.63 cm^{-1}.

The structure was solved by the heavy-atom method and refined by block-diagonal least-squares calculations with anisotropic thermal parameters. After several cycles of refinement, all hydrogen atoms were revealed in difference Fourier maps. The refinement with the weighting scheme $w = 1/|\sigma(F_o)|^2$, including the hydrogen atoms in the calculation of the structure factors, was carried to convergence. The final values of the discrepancy indexes were 0.079 for

$$R = (|F_o| - |F_c|)/\sum|F_o|$$

and 0.080 for

$$R_w = [\sum w(|F_o| - |F_c|)^2/\sum w(F_o)^2]^{1/2}$$

Atomic scattering factors and absorption coefficients were obtained from ref 7. All computations were performed on a FACOM M-190 large computer in the Data Processing Center of Kyoto University by using the program system KPAX, which included the UNICS programs.

Magnetic Susceptibility. A Faraday magnetic balance was employed for measurement of magnetic susceptibilities from 77 to 300 K. The magnetic susceptibility of anhydrous hexaamminechromium(III) chloride powder was used as a "thermometer" which was calibrated at each run to an atmospheric liquid-nitrogen temperature with corrections for the Hg barometer and gravitational constant by following the procedure of Linder.[22] The accuracy of the measurements was not less than 10%. The diamagnetic susceptibilities of the porphyrin ligand and axial ligand were corrected by measurement of free-base octaethylporphyrin and by Pascal's rule.

Results

The positional and anisotropic thermal parameters for all atoms except for hydrogen atoms are listed in Table I. A stereoscopic view of the $(OEP)Fe^{III}ClO_4$ molecule with the atomic numbering is shown in Figure 2. Agreement between chemically equivalent bond distances and angles in the core is quite satisfactory. Bond distances and angles are given in Table II. The average bond distances and angles for the four crystallographically nonequivalent pyrrole rings are presented in Figure 3. The pyrrole β-carbon–methylene carbon and the methylene carbon–methyl carbon distances for the ethyl groups are corrected for thermal motions, with the assumption that the terminal ethyl groups are "riding" on the porphinato core.

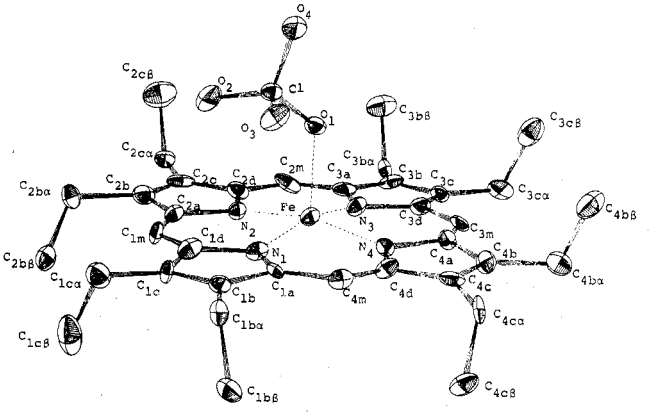

Figure 2. Computer-drawn model in perspective of the $(OEP)Fe^{III}ClO_4$ molecule. Each atom is represented by an ellipsoid having the orientation and relative size concomitant with the thermal parameters listed in Table I. The labeling scheme used for the atoms in the molecule is also shown.

As is shown in Figure 4, the porphinato core is planar within 0.04 Å. This core conformation differs from the domed and ruffled forms which have been proposed in solution by means of resonance Raman spectroscopy by Spiro et al.[21] As shown in Figure 2, the four adjacent terminal ethyl groups are oriented upward from the pyrrole planes, whereas the other four groups are downward. Although this molecular conformation is similar to that of the six-coordinated low-spin complex $(OEP)Fe^{III}(Im)_2ClO_4$,[10b] the conformation of the ethyl groups differs from those of the free base and metalloporphyrin (OEP)M (M = H_2, Ni, Zn, Ti, Ru, Co, etc.).[12] Hence, the orientation of the terminal ethyl groups seems to depend upon the molecular packing in the crystal structure. As shown in Figure 1, the crystal structure consists of dimers of $(OEP)Fe^{III}ClO_4$ molecules. The two porphyrin molecules related by a center of symmetry have "face-to-face" contact. Eight peripheral ethyl groups are wrapping the porphinato cores at the plane edge. The stacking features in the vertical views of

(12) (a) Meyer, E. F., Jr. *Acta Crystallogr., Sect. B* **1972**, *28*, 2162. (b) Cullen, D. L.; Meyer, E. F., Jr. *J. Am. Chem. Soc.* **1974**, *96*, 2095. (c) Hopf, F. R.; O'Brien, T. P.; Scheidt, W. R.; Whitten, D. G. *Ibid.* **1975**, *97*, 277. (d) Cullen, D. L.; Meyer, E. F., Jr. *Acta Crystallogr., Sect. B* **1976**, *32*, 2259. (e) Guilard, R.; Fontesse, M.; Fournari, P.; Lecomte, C.; Protas, J. *J. Chem. Soc., Chem. Commun.* **1976**, 161. (f) Little, R. G.; Ibers, J. A. *J. Am. Chem. Soc.* **1974**, *96*, 4452. (g) Lauher, J. W.; Ibers, J. A. *Ibid.* **1973**, *95*, 5148.

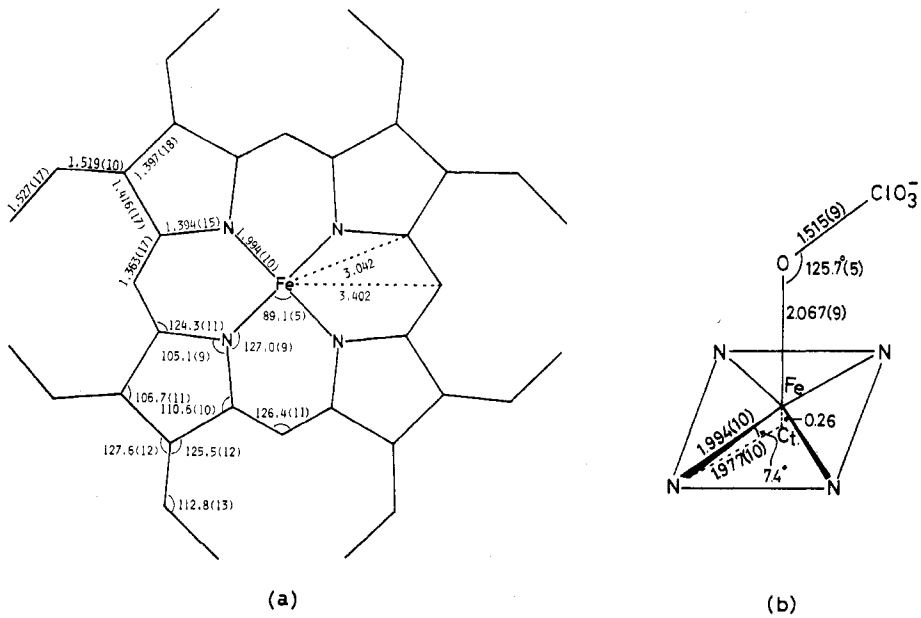

Figure 3. (a) Diagram giving the average bond distances (Å) and angles (deg) in the porphyrin skeleton of the (OEP)$Fe^{III}ClO_4$ molecule. (b) The square-pyramidal coordination group in the (OEP)$Fe^{III}ClO_4$ molecule.

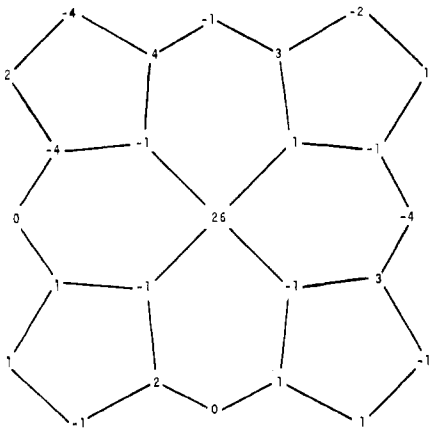

Figure 4. A formal diagram of the porphinato skeleton in (OEP)-$Fe^{III}ClO_4$ showing the perpendicular displacements, in units of 0.01 Å, from the mean plane of core. The core has the same relative orientation as Figure 2.

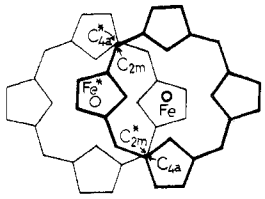

Figure 5. Stacking diagram of porphinato core for a pair of molecules approaching each other as viewed upright to the mean plane of the four porphinato nitrogen atoms.

the porphinato cores are shown in Figure 5. The distance between the mean planes defined by the four N atoms is 3.53 Å. Atomic contacts less than 4.0 Å are listed in Table III. The shortest distance (3.56 Å) is found between the meso carbon, C_{2m}, and the α-carbon of the pyrrole ring, C_{4a}*. The iron atom is situated below the pyrrole ring of the other porphyrin of the dimer. The distance from the iron to the least-squares plane including the five pyrrole ring atoms is determined to be 3.74 Å.

The perchlorate anion has approximately C_{3v} symmetry which is lower than T_d found in the free anion. Lower symmetry of coordinated ClO_4^- is rationalized by the IR spectra[13] in which the single band (1119 cm^{-1}) observed for the free anion is split into many bands.[3] As shown in Figure 2, the O_1 atom is bound to the porphinato iron as a monodentate ligand. The Cl–O_1 distance, 1.515 Å, is considerably longer than the average uncoordinated O–Cl distance, 1.411 Å. The perchlorate anion is oriented in such a manner that the O_1–Cl–O_4 plane is approximately perpendicular to the porphinato plane. The Fe–O_1 vector is almost perpendicular to the porphinato plane. The Fe–O_1 distance is 2.067 (9) Å and the Fe–O_1–Cl bond angle is 125.7 (5)°. The N_1–Fe–O_1–Cl dihedral angle is 19.02°. The Fe–O_1 distance is close to the Fe–OH_2 distance, 2.095 (2) Å, in (TPP)$Fe^{III}(OH_2)ClO_4$·2THF[6a,c] but slightly longer than Fe–$OClO_3$ in (TPP)Fe^{III}-ClO_4, 2.025 (4) Å. The Fe–O_1–Cl bond angle indicates the sp^2 character of the oxygen atom.

The geometry about the central iron is given in Figure 3b. The iron atom is displaced by 0.26 Å out of the plane defined by the four porphinato nitrogen atoms toward the ligand oxygen. The iron atom in a low-spin iron(III) porphyrin[10] usually lies in the porphinato plane, while the usual displacement of the iron from the porphinato plane in a five-coordinated high-spin porphyrin is ~0.5 Å.[5,8] Hence, the value of 0.26 Å is just intermediate between these of the extreme cases. This value is almost the same as that for (TPP)$Fe^{III}ClO_4$ reported by Scheidt and his co-workers.[6] The Fe–N distance is 1.994 (10) Å. The N–C_t distance defined by the distance between one nitrogen and the center (C_t) of the four nitrogen atoms is 1.977 (10) Å. The Fe–N distance is slightly shorter than that typical of five-coordinated high-spin derivatives (ca. 2.065 Å).[8a–c,9] The value is very close to those in low-spin derivatives.[10]

Table IV summarizes the molar susceptibility and effective magnetic moment of (OEP)$Fe^{III}ClO_4$ at temperatures from 77 to 270 K. The effective magnetic moment of (OEP)-$Fe^{III}ClO_4$ is almost the same as but lower than that of the typical low-spin state (2.15–2.74 μ_B).[23]

Discussion

Dimerization of porphyrins, as observed in (OEP)$Fe^{III}ClO_4$, has been found in a number of five-coordinate metallo-

(13) Nakamoto, K. "Infrared Spectra of Inorganic and Coordination Compounds", 2nd ed.; Wiley-Interscience: New York, 1970; pp 175–6.

Table I. Positional and Thermal Parameters for the Atoms of $(OEP)Fe^{III}ClO_4$

atom	x^a	y	z	$\beta_{11}{}^b$	β_{22}	β_{33}	β_{12}	β_{13}	β_{23}
Fe	0.4363 (1)	0.4897 (2)	0.6485 (1)	23 (1)	47 (2)	56 (1)	−3 (1)	9 (1)	0 (1)
Cl	0.3088 (1)	0.5126 (3)	0.7598 (2)	27 (1)	50 (3)	42 (2)	3 (1)	9 (1)	−5 (2)
O_1	0.3508 (4)	0.5541 (6)	0.6901 (6)	31 (3)	60 (7)	59 (6)	11 (4)	19 (3)	12 (5)
O_2	0.3550 (4)	0.4988 (8)	0.8565 (6)	41 (3)	103 (9)	58 (6)	−3 (5)	19 (3)	7 (6)
O_3	0.2788 (5)	0.4245 (9)	0.7228 (9)	43 (4)	108 (11)	158 (11)	−28 (5)	36 (5)	−33 (9)
O_4	0.2548 (5)	0.5838 (8)	0.7635 (7)	44 (4)	73 (9)	101 (8)	7 (5)	22 (4)	15 (7)
N_1	0.4653 (4)	0.3932 (8)	0.7589 (6)	17 (3)	64 (9)	29 (5)	0 (4)	−5 (3)	−1 (6)
C_{1a}	0.4317 (6)	0.3034 (10)	0.7586 (9)	30 (5)	61 (12)	64 (9)	−2 (6)	11 (5)	−1 (8)
C_{1b}	0.4605 (6)	0.2602 (9)	0.8539 (7)	26 (4)	36 (10)	29 (7)	−12 (5)	6 (4)	7 (6)
C_{1c}	0.5078 (6)	0.3232 (10)	0.9165 (8)	24 (4)	55 (11)	46 (8)	9 (5)	9 (4)	7 (7)
C_{1d}	0.5098 (6)	0.4068 (9)	0.8558 (9)	29 (4)	14 (9)	74 (9)	12 (5)	16 (5)	11 (7)
C_{1m}	0.5537 (5)	0.4869 (10)	0.8905 (7)	26 (4)	63 (11)	25 (6)	−2 (6)	0 (4)	−19 (7)
N_2	0.5175 (5)	0.5732 (7)	0.7321 (6)	25 (3)	37 (8)	38 (6)	2 (4)	2 (3)	−5 (5)
C_{2a}	0.5548 (6)	0.5577 (10)	0.8284 (8)	25 (4)	64 (12)	46 (8)	−5 (5)	9 (5)	11 (7)
C_{2b}	0.6016 (6)	0.6365 (10)	0.8697 (9)	26 (4)	55 (12)	63 (9)	23 (5)	7 (5)	1 (8)
C_{2c}	0.5889 (8)	0.7013 (12)	0.7868 (11)	45 (6)	61 (14)	83 (13)	−6 (7)	18 (7)	20 (10)
C_{2d}	0.5361 (6)	0.6656 (9)	0.7056 (8)	30 (4)	32 (11)	57 (8)	2 (5)	6 (5)	1 (7)
C_{2m}	0.5098 (6)	0.6988 (9)	0.6100 (9)	21 (4)	30 (10)	85 (10)	11 (5)	5 (5)	10 (8)
N_3	0.4272 (5)	0.5679 (8)	0.5277 (7)	24 (3)	73 (10)	48 (7)	−11 (5)	10 (4)	−17 (6)
C_{3a}	0.4594 (6)	0.6588 (10)	0.5307 (8)	21 (4)	62 (12)	45 (8)	1 (5)	4 (4)	−10 (7)
C_{3b}	0.4392 (5)	0.7020 (9)	0.4306 (8)	15 (4)	44 (11)	60 (8)	7 (5)	−4 (4)	−12 (7)
C_{3c}	0.3911 (6)	0.6412 (11)	0.3686 (9)	20 (4)	84 (13)	63 (9)	14 (6)	20 (5)	29 (8)
C_{3d}	0.3857 (6)	0.5630 (10)	0.4297 (9)	36 (5)	57 (12)	56 (8)	9 (6)	27 (5)	−23 (8)
C_{3m}	0.3444 (7)	0.4854 (10)	0.3944 (8)	51 (5)	42 (11)	36 (7)	30 (6)	−2 (5)	−7 (7)
N_4	0.3777 (5)	0.3914 (7)	0.5555 (6)	22 (3)	51 (9)	33 (6)	3 (4)	2 (3)	3 (5)
C_{4a}	0.3385 (6)	0.4065 (10)	0.4555 (9)	29 (4)	50 (12)	70 (10)	10 (6)	0 (5)	−4 (8)
C_{4b}	0.2918 (6)	0.3289 (10)	0.4153 (8)	21 (4)	85 (13)	35 (7)	20 (6)	−1 (4)	−16 (7)
C_{4c}	0.3027 (7)	0.2626 (13)	0.4955 (11)	36 (6)	99 (16)	81 (12)	8 (7)	13 (7)	−28 (11)
C_{4d}	0.3547 (6)	0.2988 (9)	0.5799 (8)	21 (4)	40 (11)	63 (8)	4 (5)	15 (5)	12 (7)
C_{4m}	0.3840 (6)	0.2660 (10)	0.6759 (8)	29 (4)	40 (11)	48 (8)	−13 (5)	10 (5)	16 (7)
$C_{1b\alpha}$	0.4376 (8)	0.1669 (11)	0.8801 (10)	52 (6)	48 (12)	79 (10)	7 (7)	18 (6)	−8 (9)
$C_{1b\beta}$	0.4779 (11)	0.0906 (13)	0.8451 (14)	97 (11)	61 (16)	133 (17)	−29 (10)	−30 (11)	16 (13)
$C_{1c\alpha}$	0.5524 (7)	0.3056 (10)	1.0234 (9)	49 (6)	43 (12)	52 (9)	−8 (6)	19 (6)	−5 (8)
$C_{1c\beta}$	0.6341 (8)	0.2757 (11)	1.0304 (11)	50 (6)	58 (13)	91 (12)	14 (7)	22 (7)	5 (10)
$C_{2b\alpha}$	0.6582 (7)	0.6510 (10)	0.9701 (9)	54 (6)	27 (11)	55 (9)	−19 (6)	20 (6)	−7 (7)
$C_{2b\beta}$	0.7269 (6)	0.5857 (12)	0.9819 (10)	27 (5)	91 (14)	71 (10)	1 (6)	7 (5)	8 (9)
$C_{2c\alpha}$	0.6244 (8)	0.7996 (12)	0.7818 (10)	54 (7)	76 (14)	72 (10)	13 (8)	22 (7)	14 (10)
$C_{2c\beta}$	0.5799 (8)	0.8752 (14)	0.7985 (12)	51 (7)	119 (18)	116 (15)	−29 (9)	35 (8)	−1 (13)
$C_{3b\alpha}$	0.4610 (7)	0.7994 (11)	0.4006 (11)	39 (6)	55 (12)	105 (12)	28 (7)	11 (7)	34 (10)
$C_{3b\beta}$	0.4169 (8)	0.8770 (14)	0.4308 (11)	46 (6)	118 (18)	88 (12)	−13 (8)	3 (7)	36 (12)
$C_{3c\alpha}$	0.3534 (7)	0.6477 (10)	0.2564 (10)	45 (6)	29 (11)	79 (10)	−3 (6)	25 (6)	11 (8)
$C_{3c\beta}$	0.2737 (8)	0.6874 (13)	0.2296 (12)	46 (7)	99 (17)	115 (14)	7 (8)	25 (8)	8 (12)
$C_{4b\alpha}$	0.2395 (7)	0.3204 (11)	0.3161 (9)	33 (5)	57 (12)	60 (9)	11 (6)	11 (5)	12 (8)
$C_{4b\beta}$	0.1632 (9)	0.3557 (16)	0.3126 (12)	54 (7)	154 (21)	91 (13)	5 (10)	6 (8)	7 (13)
$C_{4c\alpha}$	0.2710 (8)	0.1599 (10)	0.5008 (10)	60 (7)	25 (11)	63 (9)	−17 (6)	22 (7)	−16 (8)
$C_{4c\beta}$	0.3252 (7)	0.0863 (11)	0.5032 (11)	41 (5)	58 (14)	97 (12)	−9 (7)	12 (6)	−8 (10)

[a] Estimated standard deviations in the least significant figure(s) are given in parentheses. [b] The form of the anisotropic thermal parameter ellipsoid is $\exp[-(\beta_{11}h^2 + \beta_{22}k^2 + \beta_{33}l^2 + 2\beta_{12}hk + 2\beta_{13}hl + 2\beta_{23}kl)]$. The thermal parameters are multiplied by 10^4.

porphyrins.[8b,9,15,17] In contrast, dimerization of TPP-like metalloporphyrins is unlikely, due to the repulsive interaction of the bulky phenyl groups at the meso positions.[14] The π–π interactions between the "face-to-face" contact porphinato cores have been verified by X-ray studies for nickel(II) porphyrins[15] and by ESR studies on dimeric cupric and vanadyl porphyrins.[16] Such a π–π interaction is possible when the π orbitals of each porphyrin have large overlap with a pairing of a π donor and a π acceptor. The interplanar distance in $(OEP)Fe^{III}ClO_4$ is about 3.6 Å, and C_{2m} and C_{4a}* on each porphyrin core are close to each other. The interplanar distance is sufficiently short for the overlapping of the π orbitals; even with a spacing of 6.5–6.8 Å, existence of strong face-to-face interactions has been reported for the constrained *trans*-diurea binary iron(II) porphyrin by Collman et al.[18] Recent ab initio LCAO–MO calculations on porphine and its metallo derivatives[19] have shown that the two highest occupied molecular orbitals (HOMO) have A_{1u} and A_{2u} symmetries for the D_{4h} point group and that the lowest unoccupied molecular orbitals (LUMO) have E_g symmetry. These orbitals are π orbitals. The atomic orbital ϕ_{C_a} has a large coefficient in the wave function $\psi_{A_{1u}}$, and ϕ_{C_N} and ϕ_{C_m} have very large coefficients in ψ_{E_g}. The large electron density distributions at C_{4a}* for the HOMO (A_{1u}) and at C_{2m} for the LUMO (E_g) rationally permit electron transfer through π–π* interaction from C_{4a}* to C_{2m}. Therefore,the dimer of $(OEP)Fe^{III}ClO_4$ is considered to be stabilized by the π–π* interactions of the donor and acceptor. The pyrrole ring coordinates the iron atom of

(14) $(TPP)Zn^{II}ClO_4$ is only one case observed in (TPP)M in which the dimer formation would be sterically prevented by the bulky phenyl groups: Spaulding, L. D.; Eller, P. G.; Bertrand, J. A.; Felton, R. H. *J. Am. Chem. Soc.* **1974**, *96*, 982.

(15) Hamor, T. A.; Caughey, W. S.; Hoard, J. L. *J. Am. Chem. Soc.* **1965**, *87*, 2305.

(16) (a) Boyd, P. D. W.; Smith, T. D.; Price, J. H.; Pilbrow, J. R. *J. Chem. Phys.* **1972**, *56*, 1253. (b) Blumberg, W. E.; Peisach, J. *J. Biol. Chem.* **1965**, *240*, 870.

(17) (a) Cullen, D. L.; Meyer, E. F., Jr. *J. Am. Chem. Soc.* **1974**, *96*, 2095. (b) Cullen, D. L.; Meyer, E. F., Jr. *Acta Crystallogr., Sect. B* **1976**, *32*, 2259.

(18) Collman, J. P.; Elliott, C. M.; Halbert, T. R.; Tovrog, B. S. *Proc. Natl. Acad. Sci. U.S.A.* **1977**, *74*, 18.

(19) (a) Case, D. A.; Karplus, M. *J. Am. Chem. Soc.* **1977**, *99*, 6182. (b) Gouterman, M. *J. Chem. Phys.* **1959**, *30*, 1139. (c) Spangler, D.; Maggiora, G. M.; Shipman, L. L.; Christoffeerson, R. E. *J. Am. Chem. Soc.* **1977**, *99*, 7478.

Table II. Bond Distances (Å) and Angles (Deg) for $(OEP)Fe^{III}ClO_4$

$Fe-N_1$ [a]	1.997 (10) [b]	$C_{4c\alpha}-C_{4c\beta}$	1.47 (1)	$N_3C_{3a}C_{2m}$	127 (1)
$Fe-N_2$	2.022 (10)	$Cl-O_1$	1.52 (1)	$C_{3b}C_{3a}C_{2m}$	121 (1)
$Fe-N_3$	1.954 (11)	$Cl-O_2$	1.38 (1)	$N_3C_{3d}C_{3c}$	115 (1)
$Fe-N_4$	2.002 (10)	$Cl-O_3$	1.41 (1)	$N_3C_{3d}C_{3m}$	121 (1)
$Fe-O_1$	2.067 (9)	$Cl-O_4$	1.45 (1)	$C_{3c}C_{3d}C_{3m}$	124 (1)
N_1-C_{1a}	1.42 (2)			$N_4C_{4a}C_{4b}$	112 (1)
N_1-C_{1d}	1.37 (1)	N_1FeN_2	88.3 (5)	$N_4C_{4a}C_{3m}$	127 (1)
N_2-C_{2a}	1.33 (1)	N_1FeN_3	165.3 (4)	$C_{4b}C_{4a}C_{3m}$	122 (1)
N_2-C_{2d}	1.42 (2)	N_1FeN_4	89.3 (5)	$N_4C_{4d}C_{4c}$	109 (1)
N_3-C_{3a}	1.42 (2)	N_2FeN_3	91.1 (5)	$N_4C_{4d}C_{4m}$	118 (1)
N_3-C_{3d}	1.35 (1)	N_2FeN_4	165.1 (4)	$C_{4c}C_{4d}C_{4m}$	133 (1)
N_4-C_{4a}	1.38 (1)	N_3FeN_4	87.6 (5)	$C_{1a}C_{1b}C_{1c}$	108 (1)
N_4-C_{4d}	1.45 (2)	N_1FeO_1	99.7 (4)	$C_{2a}C_{2b}C_{2c}$	104 (1)
$C_{1a}-C_{1b}$	1.40 (2)	N_2FeO_1	96.5 (5)	$C_{3a}C_{3b}C_{3c}$	106 (1)
$C_{1c}-C_{1d}$	1.45 (2)	N_3FeO_1	95.0 (5)	$C_{4a}C_{4b}C_{4c}$	106 (1)
$C_{2a}-C_{2b}$	1.44 (2)	N_4FeO_1	98.4 (5)	$C_{1b}C_{1c}C_{1d}$	107 (1)
$C_{2c}-C_{2d}$	1.37 (2)	O_1ClO_2	111.7 (5)	$C_{2b}C_{2c}C_{2d}$	109 (1)
$C_{3a}-C_{3b}$	1.48 (2)	O_1ClO_3	110.4 (6)	$C_{3b}C_{3c}C_{3d}$	106 (1)
$C_{3c}-C_{3d}$	1.41 (2)	O_1ClO_4	104.2 (6)	$C_{4b}C_{4c}C_{4d}$	108 (1)
$C_{4a}-C_{4b}$	1.42 (2)	O_2ClO_3	107.6 (7)	$C_{1d}C_{1m}C_{2a}$	121 (1)
$C_{4c}-C_{4d}$	1.39 (2)	O_2ClO_4	109.4 (6)	$C_{2d}C_{2m}C_{3a}$	128 (1)
$C_{1b}-C_{1c}$	1.38 (2)	O_3ClO_4	114.6 (6)	$C_{3d}C_{3m}C_{4a}$	124 (1)
$C_{2b}-C_{2c}$	1.43 (2)	FeN_1C_{1a}	125.7 (6)	$C_{4d}C_{4m}C_{1a}$	133 (1)
$C_{3b}-C_{3c}$	1.36 (2)	FeN_1C_{1d}	126.8 (8)	$C_{1a}C_{1b}C_{1b\alpha}$	124 (1)
$C_{4b}-C_{4c}$	1.42 (2)	FeN_2C_{2a}	125.0 (8)	$C_{1c}C_{1b}C_{1b\alpha}$	128 (1)
$C_{1d}-C_{1m}$	1.41 (2)	FeN_2C_{2d}	126.6 (8)	$C_{1b}C_{1c}C_{1c\alpha}$	126 (1)
$C_{2a}-C_{1m}$	1.32 (2)	FeN_3C_{3a}	123.6 (7)	$C_{1d}C_{1c}C_{1c\alpha}$	127 (1)
$C_{2d}-C_{2m}$	1.35 (2)	FeN_3C_{3d}	134.2 (10)	$C_{2a}C_{2b}C_{2b\alpha}$	132 (1)
$C_{3a}-C_{2m}$	1.35 (2)	FeN_4C_{4a}	124.8 (9)	$C_{2c}C_{2b}C_{2b\alpha}$	124 (1)
$C_{3d}-C_{3m}$	1.36 (2)	FeN_4C_{4d}	129.4 (9)	$C_{2b}C_{2c}C_{2c\alpha}$	129 (1)
$C_{4a}-C_{3m}$	1.42 (2)	$C_{1a}N_1C_{1d}$	106 (1)	$C_{2d}C_{2c}C_{2c\alpha}$	122 (1)
$C_{4d}-C_{4m}$	1.36 (2)	$C_{2a}N_2C_{2d}$	108 (1)	$C_{3a}C_{3b}C_{3b\alpha}$	128 (1)
$C_{1a}-C_{4m}$	1.34 (2)	$C_{3a}N_3C_{3d}$	102 (1)	$C_{3c}C_{3b}C_{3b\alpha}$	126 (1)
$C_{1b}-C_{1b\alpha}$	1.49 (2)	$C_{4a}N_4C_{4d}$	105 (1)	$C_{3b}C_{3c}C_{3c\alpha}$	130 (1)
$C_{1c}-C_{1c\alpha}$	1.49 (1)	FeO_1Cl	125.7 (5)	$C_{3d}C_{3c}C_{3c\alpha}$	124 (1)
$C_{2b}-C_{2b\alpha}$	1.50 (1)	$N_1C_{1a}C_{1b}$	109 (1)	$C_{4a}C_{4b}C_{4b\alpha}$	128 (1)
$C_{2c}-C_{2c\alpha}$	1.56 (1)	$N_1C_{1a}C_{4m}$	123 (1)	$C_{4c}C_{4b}C_{4b\alpha}$	126 (1)
$C_{3b}-C_{3b\alpha}$	1.56 (3)	$C_{1b}C_{1a}C_{4m}$	127 (1)	$C_{4b}C_{4c}C_{4c\alpha}$	132 (1)
$C_{3c}-C_{3c\alpha}$	1.51 (1)	$N_1C_{1d}C_{1c}$	109 (1)	$C_{4d}C_{4c}C_{4c\alpha}$	119 (1)
$C_{4b}-C_{4b\alpha}$	1.45 (1)	$N_1C_{1d}C_{1m}$	126 (1)	$C_{1b}C_{1b\alpha}C_{1b\beta}$	112 (1)
$C_{4c}-C_{4c\alpha}$	1.60 (1)	$C_{1c}C_{1d}C_{1m}$	125 (1)	$C_{1c}C_{1c\alpha}C_{1c\beta}$	113 (1)
$C_{1b\alpha}-C_{1b\beta}$	1.49 (1)	$N_2C_{2a}C_{2b}$	111 (1)	$C_{2b}C_{2b\alpha}C_{2b\beta}$	112 (1)
$C_{1c\alpha}-C_{1c\beta}$	1.60 (2)	$N_2C_{2a}C_{1m}$	132 (1)	$C_{2c}C_{2c\alpha}C_{2c\beta}$	113 (1)
$C_{2b\alpha}-C_{2b\beta}$	1.59 (2)	$C_{2b}C_{2a}C_{1m}$	117 (1)	$C_{3b}C_{3b\alpha}C_{3b\beta}$	112 (1)
$C_{2c\alpha}-C_{2c\beta}$	1.42 (1)	$N_2C_{2d}C_{2c}$	108 (1)	$C_{3c}C_{3c\alpha}C_{3c\beta}$	115 (1)
$C_{3b\alpha}-C_{3b\beta}$	1.52 (1)	$N_2C_{2d}C_{2m}$	121 (1)	$C_{4b}C_{4b\alpha}C_{4b\beta}$	114 (1)
$C_{3c\alpha}-C_{3c\beta}$	1.59 (3)	$C_{2c}C_{2d}C_{2m}$	130 (1)	$C_{4c}C_{4c\alpha}C_{4c\beta}$	113 (1)
$C_{4b\alpha}-C_{4b\beta}$	1.55 (4)	$N_3C_{3a}C_{3b}$	111 (1)		

[a] The atoms respectively noted by the labelings given in Figure 2. [b] The numbers in parentheses are the estimated standard deviations in the last significant figures.

Table III. Packing Distances in the Crystalline Arrangement

bond type	length, Å	bond type	length, Å
$Fe-C_{3b}$* [a]	3.936 (14)	$C_{2m}-C_{3m}$*	3.809 (20)
$Fe-C_{3c}$*	3.813 (13)	$C_{2m}-N_4$*	3.728 (17)
$Fe-C_{3d}$*	3.868 (14)	$C_{2m}-C_{4a}$*	3.557 (19)
N_1-C_{3b}*	3.786 (16)	$C_{2m}-C_{4b}$*	3.874 (17)
N_1-C_{3c}*	3.635 (16)	N_3-N_3*	3.603 (15)
N_2-C_{3c}*	3.929 (19)	N_3-C_{3d}*	3.889 (16)
N_2-C_{3d}*	3.765 (17)	$C_{3a}-N_4$*	3.653 (16)
N_2-C_{3m}*	3.597 (17)	$C_{3a}-C_{4a}$*	3.880 (17)
$C_{2d}-C_{3m}$*	3.639 (20)	$C_{3b}-N_4$*	3.657 (14)
$C_{2d}-C_{4a}$*	3.790 (19)	$C_{3b}-C_{4d}$*	3.931 (16)

[a] The atoms with asterisk belong to molecule related by the center of symmetry at $^1/_2$, $^1/_2$, $^1/_2$.

Table IV. Molar Susceptibilities and Effective Magnetic Moments at Some Temperatures

T, K	$10^6\chi_M$ [a]	μ_{eff}, μ_B	T, K	$10^6\chi_M$ [a]	μ_{eff}, μ_B
77.2	28 000	4.16	190	13 100	4.46
83.6	26 400	4.20	201	12 700	4.52
97.2	23 000	4.23	211	12 200	4.53
107	20 500	4.20	222	11 800	4.58
120	18 800	4.25	233	11 500	4.64
131	17 300	4.26	242	11 100	4.64
144	16 000	4.30	254	10 800	4.68
156	15 100	4.35	264	10 600	4.73
166	14 300	4.35	275	10 400	4.78
177	13 600	4.39			

[a] χ_M in cgsu.

the counterpart porphyrin as a weak sixth ligand. $\pi-\pi$ interactions as observed in (π-pyrrolyl)iron and (π-pentadienyl)iron[20] may also be possible between the iron and the pyrrole ring. The existence of these $\pi-\pi$ interactions between $(OEP)Fe^{III}ClO_4$ molecules may contribute to retention of the core planarity in the crystal. Although the asymmetric five-coordination may cause the doming or ruffling form of the core as observed in solution,[21] the OEP core of the complex shows

(20) Moffitt, W. *J. Am. Chem. Soc.* **1954**, *76*, 3386.

(21) (a) Spiro, T. G.; Stong, J. D.; Stein, P. *J. Am. Chem. Soc.* **1979**, *101*, 2648. (b) Rakshit, G.; Spiro, T. G. *Biochemistry* **1974**, *13*, 5317. (c) Spiro, T. G.; Strekas, T. C. *J. Am. Chem. Soc.* **1974**, *96*, 338.

(22) Linder, C. T. Research Report R-94433-2-A (Westinghouse Research Laboratories).

the intact planar structure in the crystalline state.

As described in the Introduction, we are particularly interested in the spin state of the iron. The iron in the established structure has four strong-field planar ligands, porphines, and a weak-field axial ligand, perchlorate. From the viewpoint of ligand field theory, the structure allows the $3d^5$ energy levels to split to $d_{x^2-y^2}$ and d_{z^2} of d_σ antibonding orbitals and d_{xy}, d_{yz}, and d_{zx} of d_π bonding orbitals. The d_{z^2} orbital energy is lower than the $d_{x^2-y^2}$ energy because of a weak axial ligand (the perchlorate anion). The d_{z^2} level would be further lowered by the weak bonding of the lone pair of the perchlorate oxygen, while the interorbital interaction between the antibonding π^* of the oxygen and the d_{yz} and d_{zx} of the iron may cause effective Fe→(O–Cl) π^* back-bonding. In the established perchlorate structure, the Cl–O_1 bond is longer than the other three Cl–O bonds. The longer Cl–O_1 bond must give evidence of Fe→(O–Cl) π^* back-bonding. Although this interaction stabilizes the d_{yz} and d_{zx} orbitals, these d_{yz} and d_{zx} orbitals must be raised due to the repulsion by the $2p_z$ electrons of the equatorial ligand nitrogens, while the d_{xy} orbital interacts directly neither with the equatorial nitrogens nor with the axial oxygen. Thus the d_{xy} orbital energy will be lower than that for the d_{yz} and d_{zx} orbitals. The Fe–N distances and the size of the central hole of the porphinato core are strongly related to the occupancy of the $d_{x^2-y^2}$ orbital.[5] If the nitrogen comes near the central iron in the equatorial direction, the $d_{x^2-y^2}$ orbital energy would be raised because of repulsion between the $d_{x^2-y^2}$ electron and the sp^2 lone-pair electrons of the nitrogen. When the energy gap between the $d_{x^2-y^2}$ and d_{z^2} levels exceeds the pairing energy, the raised $d_{x^2-y^2}$ orbital is unoccupied. Consequently, the nonoccupancy of the $d_{x^2-y^2}$ orbital results in shorter Fe–N distance. The Fe–N distances of the complex are shorter than the C_t–N distance observed in metal-free OEP (2.062 Å).[12g] The value is very close to those in the low-spin derivatives possess vacant $d_{x^2-y^2}$ orbitals.[10] Therefore, the $d_{x^2-y^2}$ orbital of the intermediate-spin complex is thought to be unoccupied. The displacement of the iron from the porphinato plane is associated with occupancy of the d_{z^2} orbital. Since the displacement of 0.26 Å is intermediate between those of low spin[10] and the high spin,[5,8] the d_{z^2} orbital may be singly occupied. An intermediate value for the displacement of the iron seems to be characteristic of the pentacoordinate intermediate-spin ($S = {}^3/_2$) complex. The ground-state configuration is expressed by the configuration $(d_{xy})^2(d_{yz})(d_{zx})(d_{z^2})$. Indeed, the geometric parameters of the studied $(OEP)Fe^{III}ClO_4$ are very similar to those of $(TPP)Fe^{III}ClO_4$ (Fe–C_t = 0.27 Å, Fe–N = 1.997 Å),[6] which has been presumed to have the same configuration as $(OEP)Fe^{III}ClO_4$, and also those of the high-spin d^4 $(TPP)Mn^{II}Cl$ (Mn–C_t = 0.265 Å, Mn–N = 2.008 Å),[11] which has a singly occupied $3d_{z^2}$ and an unoccupied $3d_{x^2-y^2}$ orbital. In the Mössbauer spectra of $(OEP)Fe^{III}ClO_4$, the large positive quadrupole splitting indicates that the energy levels of the singly occupied d_{yz} and d_{zx} states are higher than that of the doubly occupied d_{xy} state.[4] The complex has almost the same effective magnetic moments $\mu_{eff} = 4.2\ \mu_B$ at 77 K and $4.7\ \mu_B$ at 275 K. When these values are compared with calculated values $\mu_{eff} = 5.92$, 3.87, and $1.73\ \mu_B$ for $S = {}^5/_2$, ${}^3/_2$, and ${}^1/_2$, respectively, the complex can be regarded as an intermediate-spin ($S = {}^3/_2$) complex.[2,4] It is noted that the $(TPP)Fe^{III}ClO_4$ crystal recently studied by Scheidt et al. included *m*-xylene.[6b] The mean separation of *m*-xylene from the porphinato core was determined as 3.48 Å, which is close to that of the separation of the paired $(OEP)Fe^{III}ClO_4$. The *m*-xylene molecule is thought to act as a π base to stabilize $(TPP)Fe^{III}ClO_4$ in the crystalline state. This fact indicates that the pyrrole ring of the OEP core coordinates axially to the iron as a π base to stabilize the $(OEP)Fe^{III}ClO_4$ structure.

As described so far, the $S = {}^3/_2$ state only of $(OEP)Fe^{III}ClO_4$ could be assigned from its structural properties. Thus, it is concluded that the Fe–N and Fe–C_t distances can be used as good structural indicators to determine the relative energy levels and/or the occupancy of the $d_{x^2-y^2}$ and d_{z^2} orbitals of (porphinato)iron complexes.

When we compare the spectroscopic properties of ferricytochrome *c′* with those of the intermediate-spin complexes, there are many similarities. Since the intermediate-spin state of $(OEP)Fe^{III}ClO_4$ resulted from the weak bonding of the perchlorate group to the iron, the histidyl imidazole at the proximal site of ferricytochrome *c′* would weakly coordinate the heme. That is, the proximal imidazole nitrogen might be bound to the iron as a weak ligand due to the conformation of the apoprotein at physiological pH values.

In order to reveal more precisely the structural features for intermediate-spin (porphinato)iron(III), we are proceeding with structure analyses of new ferric complexes possessing anomalous spin states.[3,4]

Acknowledgment. We thank Professor Hiroshi Kato for his helpful comments concerning the theoretical interpretation.

Registry No. $(OEP)Fe^{III}ClO_4$, 50540-30-2.

Supplementary Material Available: Listing of structure factor amplitudes (14 pages). Ordering information is given on any current masthead page.

(23) (a) Epstein, L. M.; Straub, D. K.; Maricondi, C. *Inorg. Chem.* **1967**, *6*, 1720. (b) Bullard, L.; Panayappan, R.; Thorpe, A.; Hambright, P.; Ng, G. *Bioinorg. Chem.* **1973**, *3*, 41.